

Original Article

Inhibitory effects of metastin on migration and invasion of human nasopharyngeal carcinoma cells

Qijun Jing^{1,2*}, Zelai He^{1,2*}, Hongbo Xu^{1,2}, Qian Sun^{1,2}, Gengming Wang^{1,2}, Yan Zhou^{1,2}, Hao Jiang^{1,2}

¹Department of Radiation Oncology, The First Affiliated Hospital of Bengbu Medical College and Tumor Hospital Affiliated to Bengbu Medical College, 287 Changhuai Road, Bengbu 233004, Anhui, P. R. China; ²Anhui Province Key Laboratory of Translational Cancer Research Affiliated to Bengbu Medical College, Bengbu 233004, Anhui, P. R. China. *Equal contributors.

Received March 25, 2019; Accepted June 10, 2019; Epub August 15, 2019; Published August 30, 2019

Abstract: The objective of the current study was to investigate the inhibitory effects of metastin (also known as kisspeptin) on migration and invasion abilities of human nasopharyngeal carcinoma (NPC) SUNE-1-5-8F cells. Transwell migration assays were used to examine the effects of different concentrations of metastin on migration and invasion abilities of SUNE-1-5-8F cells. The effects of metastin on rates of inhibition, metastatic inhibition, and survival were further examined in the BALB/c-nu mouse model of lung metastasis. Kisspeptin expression in pulmonary metastatic foci was observed by immunohistochemistry. Metastin displayed significant inhibitory effects on migration and invasion abilities of SUNE-1-5-8F cells, in a dose-dependent manner ($p < 0.05$). In the nude mouse model, metastin failed to inhibit tumor cell proliferation, but suppressed lung metastasis ($p < 0.05$) and prolonged survival times ($p < 0.05$). Immunohistochemistry results indicated that kisspeptin expression was higher in the metastin treatment group than the control group. In summary, metastin has the potential to inhibit migration and invasion of nasopharyngeal carcinoma cells.

Keywords: Metastin, nasopharyngeal carcinoma, migration, invasion

Introduction

Nasopharyngeal carcinoma (NPC), defined as cancer of the head and neck, is common in China, especially in South China. NPC is characterized by high malignancy, spatial aggregation, and metastasis [1]. NPC generally occurs in regions with complex anatomical relationships. Non-keratinized squamous cell carcinoma is the dominant pathological type. NPC is sensitive to radiotherapy, the first-line treatment for NPC. Failed radiotherapy for NPC is often associated with localized non-response and distant metastasis [2]. Intensity modulated radiotherapy has greatly increased the localized control of NPC, but distant metastasis remains the major reason of failed treatment. Inhibiting distant metastasis is very important in increasing 5-year survival rates of NPC patients.

Metastin (also known as kisspeptin) is a protein encoded by the metastasis suppressor ge-

ne KISS-1 in humans. A ligand for human orphan G-protein-coupled receptor (HOT7T175 or GPR54) [3, 4], metastin provides inhibitory effects on metastasis and invasion of various tumor cells, including colorectal cancer [5], renal cancer [6], breast cancer [7], and thyroid cancer [8] cells. However, its roles in NPC remain unknown. The current study investigated potential inhibitory effects of different concentrations of metastin on invasion and migration abilities of human NPC SUNE-1-5-8F cells.

Materials and methods

Materials and equipment

Metastin (KISS-1 68-121) was purchased from Sigma (USA). Other reagents included PRMI 1640 medium, penicillin-streptomycin, phosphate buffer saline (PBS) (Hyclone), 0.25% trypsin, crystal violet staining solution (Beyotime), fetal bovine serum (Sijiqing), BD Matrigel matrix, and Transwell supports (24 wells, 8.0 μ m

Metastin inhibits migration and invasion of nasopharyngeal carcinoma cells

pore size, Corning). A medical double-person double-side clean bench (SW-CJ-2F) (Suzhou Purification Equipment Factory, China), Thermo 3111 incubator (Thermo, USA), MDF-192 refrigerator (SANYO, Japan), Olympus CKX41 inverted phase-contrast microscope (Olympus, Japan), Eppendorf centrifuge 5810R (Eppendorf, Germany), and H-SWX-60085 water bath (Shanghai CIMO Medical Instrument Co., Ltd.) were also obtained.

A total of forty 4-week-old female BALB/c-nu mice (license number 201603475) were purchased from the Comparative Medicine Centre of Yangzhou University. They were bred in a barrier environment at the Center of Laboratory Animals, Bengbu Medical College. All animal studies were reviewed and approved by the "Animal Care and Use Committee of Bengbu Medical College". The SUNE-1-5-8F cell line (human NPC) was purchased from GuangZhou Jennio Biotech Co., Ltd. [9, 10].

Cell resuscitation and culturing

Frozen cells were removed from the -80°C MDF-192 refrigerator and thawed in a 37°C water bath, with gentle shaking. The cell suspension (~ 1 mL) was transferred to a centrifuge tube and an appropriate amount of culture medium (PRMI 1640 medium containing 15% FBS and 1% penicillin-streptomycin) was added. This was followed by mixing. The cells were centrifuged at 1,000 rpm and 4°C for 5 minutes. The supernatant was discarded and the cells were resuspended in 1 mL of culture medium. After gentle blowing and mixing, the cells were transferred to a culture flask containing 4 mL of culture medium. They were then placed in a 5% CO_2 incubator at 37°C [11].

Transwell migration assays

Migration assay: The culture flask was taken out and the culture medium was discarded. The cells were digested with 1 mL of 0.25% trypsin for 1 minute, then resuspended in 1 mL of culture medium. The suspension was transferred to a centrifuge tube and centrifuged at 4°C and 1,000 rpm for 5 minutes. The supernatant was discarded and the cells were counted. Next, 50×10^3 SUNE-1-5-8F cells were added into the upper chamber of the Transwell unit. Different concentrations of metastin (10^2 nM, 10^3 nM, and 10^4 nM), prepared using 200 μl of PRMI 1640 medium, were added into the upper

chamber for the test groups. PRMI 1640 medium, alone, at an identical volume was used for the control group. In the lower chamber, 800 μl of PRMI 1640 medium containing 15% FBS was added. The cells were cultured in the incubator for 24 hours. Cells that did not migrate through the membrane were removed with a cotton swab. Cells that migrated were fixed in 4% paraformaldehyde for 30 minutes, washed with PBS twice, and stained with crystal violet for 30 minutes. After washing with PBS twice, the cells were observed under a microscope (magnification, $\times 200$). For each membrane, five fields of view were randomly selected. The cells were counted and photographed. An average cell count was then taken [12].

Invasion assay: Briefly, 200 μl pipette tips, PRMI 1640 medium, and Matrigel were pre-cooled at 4°C for 30 minutes. The dilution was prepared using pre-cooled Matrigel and PRMI 1640 medium at a ratio of 1:5, mixing properly. The upper chamber was coated with 50 μl of the diluted Matrigel and placed in the incubator for 1 hour. The culture flask was taken out and the culture medium was discarded. The cells were digested with 1 mL of 0.25% trypsin for 1 minute, then resuspended in 1 mL of culture medium. The cells were centrifuged at 1,000 rpm and 4°C for 5 minutes. The supernatant was discarded and the cells were counted. Next, 50×10^3 SUNE-1-5-8F cells were added into the upper chamber of the Transwell unit. Different concentrations of metastin (10^2 nM, 10^3 nM, and 10^4 nM), prepared in 200 μl of PRMI 1640 medium, were added into the upper chamber for the test groups. An identical volume of PRMI 1640 medium, alone, was added into the upper chamber for the control group. In the lower chamber, 800 μl of PRMI 1640 medium containing 15% FBS was added. After incubating the cells for 24 hours, cells that did not pass through the Matrigel were removed with a cotton swab. The cells were fixed in 4% paraformaldehyde for 30 minutes, washed with PBS twice, stained with crystal violet for 30 minutes, and washed with PBS twice before examination under a microscope (magnification, $\times 200$). For each membrane, five fields of view were randomly selected. The cells were counted and photographed. An average cell count was taken.

Concentrations of metastin were chosen, according to previously published reports. How-

Metastin inhibits migration and invasion of nasopharyngeal carcinoma cells

ever, a preliminary experiment was conducted, assessing effective concentrations. Concentrations of 10^2 nM, 10^3 nM, and 10^4 nM were finally chosen [13].

Tumor transplantation experiment in nude mice

Log-phase SUNE-1-5-8F cells were harvested and a cell suspension was prepared using 0.9T normal saline. The cell concentration was adjusted to 2×10^6 /mL, then 0.2 mL of the cell suspension was injected into the right axillary region of the nude mice [14]. The mice were randomly divided into metastin treatment and control groups, with 20 mice in each group. Nude mice were bred in a specific pathogen free (SPF) environment, in strict accordance with SPF protocol. For the test group, metastin was administered intraperitoneally at a dose of 1.17 mg/kg the day after tumor transplantation. The control group did not receive metastin. After implanting the tumor cells, this study measured the longest diameter (highest longitudinal diameter) and width (highest transverse diameter) of subcutaneous tumors *in vivo* using an external caliper and the blind method. The longest diameter and width were measured three times for each direction, respectively. The average value was calculated, determining the longest diameter and width. Tumor volume was calculated as follows: tumor volume = (length \times width²)/2. Tumor volume was determined once every 5 days.

Endpoint criteria: Mice with a body weight loss of 15% were sacrificed using cervical dislocation, aiming to reduce the time of animal suffering [15, 16]. Other animal endpoint criteria included dehydration greater than 10%, restricted motor function by the engrafted tumor, and moribund behavior.

Tumor inhibition rates and tumor burden

Ten mice were randomly selected from each group on day 30. The mice (~20-25 g) were sacrificed by cervical dislocation. After the subcutaneous tumors were dissected, they were weighed using an electronic scale [17]. Tumor mass inhibition rates (%) were calculated as follows: Tumor mass inhibition rate (%) = (the average tumor mass of the control group - average tumor mass of the metastin treatment group) / the average tumor mass of the control group

$\times 100\%$. Subcutaneous tumor burden is expressed as a percentage of the tumor mass versus the body weight [14, 18].

Counting of lung metastatic foci and determining metastasis inhibition rates

Lung metastatic tumors have been considered the standard of metastatic assessment, as the lungs are the primary organs of metastasis for nasopharyngeal carcinoma. They are easy to dissect and observe [19-21]. Given the clinical significance and scientific rigor of this type of tumor, lung metastatic tumors are the standard for assessment of metastasis [19-22].

On day 30, the mice were sacrificed. Tumor tissues were fixed in 10% formaldehyde. Metastatic foci stained a lighter color than healthy lung tissues, with smooth margins and quasi-circular nodules. This study observed and counted the lung surface pulmonary nodules, front and back pulmonary nodules, and interlobar region of pulmonary nodules. Inhibition rates of metastatic lung tumors (%) were calculated as follows: Tumor metastasis inhibition rate (%) = (the average number of metastatic lung tumors in the control group - the average number of metastatic lung tumors in the metastin treatment group) / the average number of metastatic lung tumors in the control group $\times 100\%$. After counting, the tissues were fixed in 10% formaldehyde, dehydrated, and embedded in paraffin [23]. The sections were used for pathological and immunohistochemical studies.

Survival analysis

Survival curves were obtained by observing the number of the remaining mice. Mean survival times (MST, days) were calculated and survival prolongation rates (%) were calculated as follows: Survival prolongation rate (%) = (MST in metastin treatment group - MST in the control group) / MST in the control group $\times 100\%$ [17, 24].

Hematoxylin-eosin staining and immunohistochemical staining

Lung metastatic foci were fixed in 10% formaldehyde, dehydrated, and embedded in paraffin. Tissue blocks were sectioned at a thickness of 4 μ m. Hematoxylin-eosin staining and

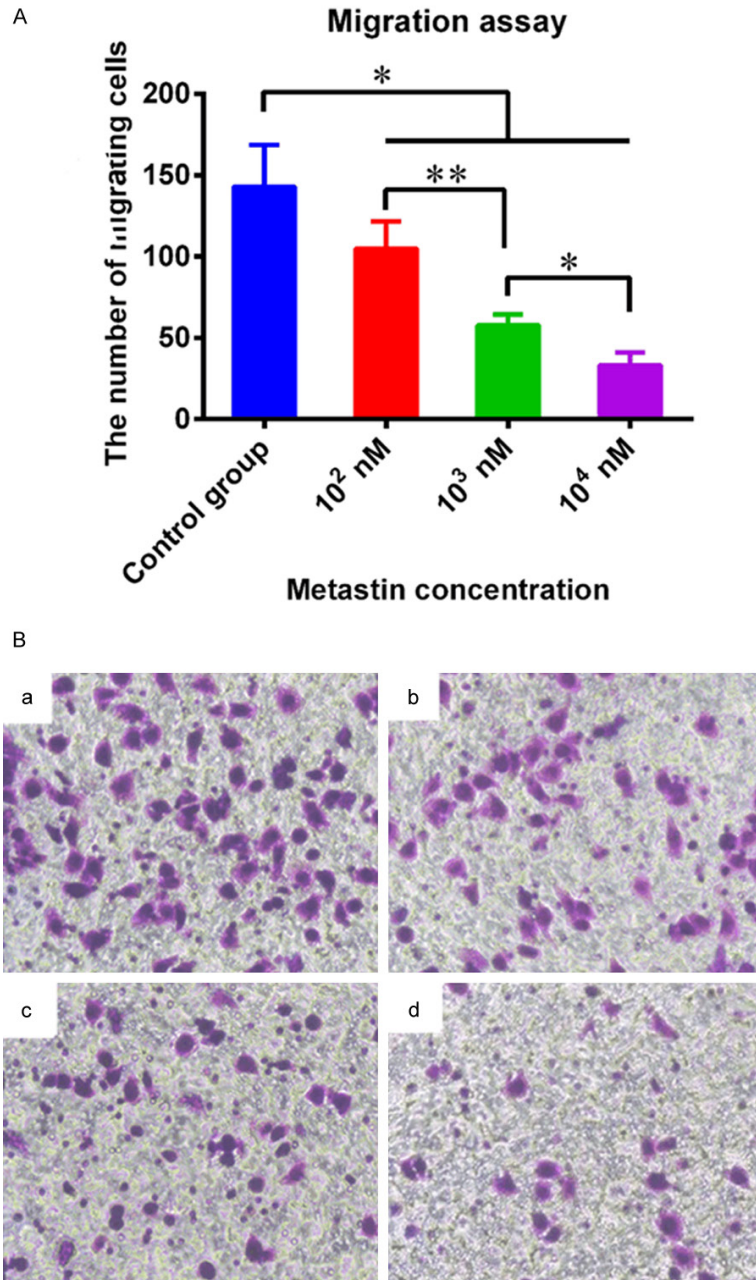


Figure 1. A. Comparison of the number of migrating tumor cells after treatment with different concentrations of metastin. There were significant differences in tumor cell migration between the test and control groups and there were also significant differences among the different dose groups; B. Migration of SUNE-1-5-8F cells after treatment with different concentrations of metastin (magnification, 200 ×). a: Control; b: 10² nM metastin group; c: 10³ nM metastin group; d: 10⁴ nM metastin group. *indicates $p < 0.05$; **indicates $p < 0.01$.

immunohistochemical staining were performed in the Pathology Department, First Affiliated Hospital of Bengbu Medical College. Kisspeptin expression in immunohistochemically stained

tissue cross-sections was determined by observing the proportion of positive cells among all cells and staining intensity levels of positive cells [13].

A: Score based on the proportion of positive cells. Positive cells $< 1/3$, 1; $1/3 < \text{positive cells} < 2/3$, 2; Positive cells $> 2/3$, 3. B: Score based on the staining intensity of positive cells. Negative cells, 0; Pale blue cells, 1; Deep blue cells, 2; Purple blue cells, 3. Final scores = A*B. "A*B = 0" was determined as (+); "A*B = 3-4" was determined as (++) ; "A*B = 6-9" was determined as (+++).

Statistical analysis

Measurements are expressed as mean \pm standard deviation. For the *in vitro* experiment, each group had at least three replications. For the *in vivo* experiment, each group had at least seven mice. IBM SPSS Statistics 19 software (IBM Corporation, Chicago, USA) was used for analysis. Comparisons of the two groups were performed using one-way analysis of variance (ANOVA) and Tukey's post-hoc tests. Survival curve were obtained via Kaplan-Meier survival analysis and compared using log-rank tests. $P < 0.05$ indicates significant differences.

Results

Transwell migration assay

After metastin intervention, migration of tumor cells was inhibited significantly, compared with that of the control cells ($p < 0.05$). As the concentration of metastin increased, the migration of tumor cells decreased considerably (**Figure 1A, 1B**).

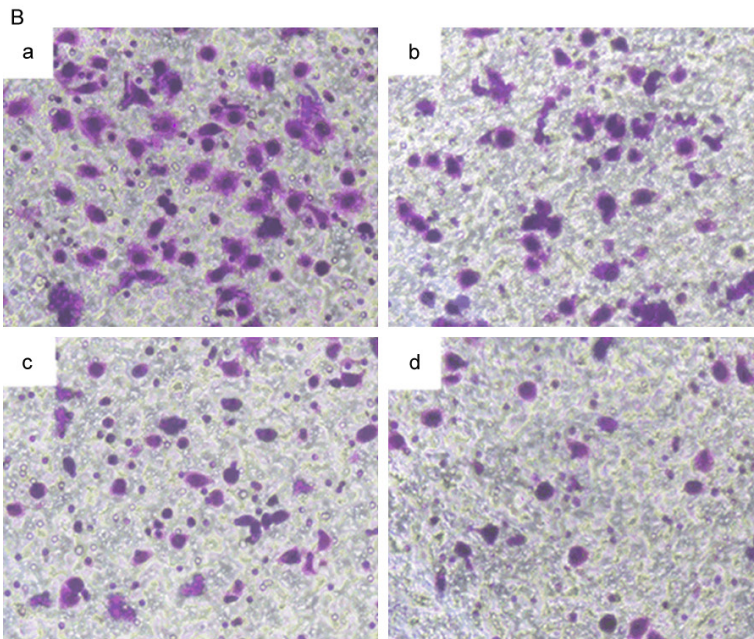
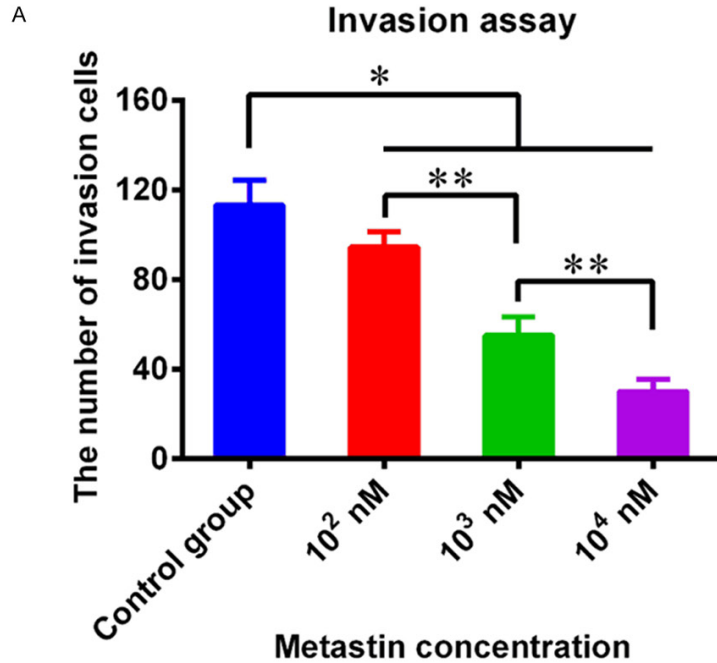


Figure 2. A. Comparison of the number of invading tumor cells after treatment with different concentrations of metastin. There were significant differences in tumor cell invasion between the test and control groups and there were also significant differences among the different dose groups; B. Invasion of SUNE-1-5-8F cells after treatment with different concentrations of metastin (magnification, 200 ×). a: Control group; b: 10² nM metastin group; c: 10³ nM metastin group; d: 10⁴ nM metastin group. *indicates $p < 0.05$; **indicates $p < 0.01$.

Transwell invasion assay

After metastin intervention, invasion of tumor cells was significantly inhibited, compared with

that of the control cells ($p < 0.05$). As the concentration of metastin increased, the invasion of tumor cells considerably decreased (Figure 2A, 2B).

Inhibitory effects of metastin on axillary transplanted tumors in nude mice

Subcutaneous tumors were observed in all mice after tumor transplantation on day 30. Average tumor volume and mass values were obtained. The final tumor volume and mass values were 1.14 cm³ and 1.47 g for the control group and 0.92 cm³ and 1.41 g for the test group, respectively (Figure 3A, 3B). Compared to the negative control group, the tumor mass inhibition rate of the test group was 4.48%. No significant differences were found in subcutaneous tumor volume and mass between the two groups (Figure 3A, 3B). On the other hand, the maximum tumor burden was 10.56% and the minimum tumor burden was 4.23% in the negative control group. The maximum tumor burden was 8.94% and the minimum tumor burden was 3.75% in the test group. The mean tumor burden was 6.25% in the negative control group and 5.18% in the test group. Additionally, there were no significant differences in tumor burden between negative control and test groups.

Inhibitory effects of metastin on lung metastatic foci after inoculation of SUNE-1-5-8F cells

After sacrificing the mice, the lungs were harvested and fixed in 10% formaldehyde. The number of lung metastatic tumors, as well as the diameter of each tumor, was determined

Metastin inhibits migration and invasion of nasopharyngeal carcinoma cells

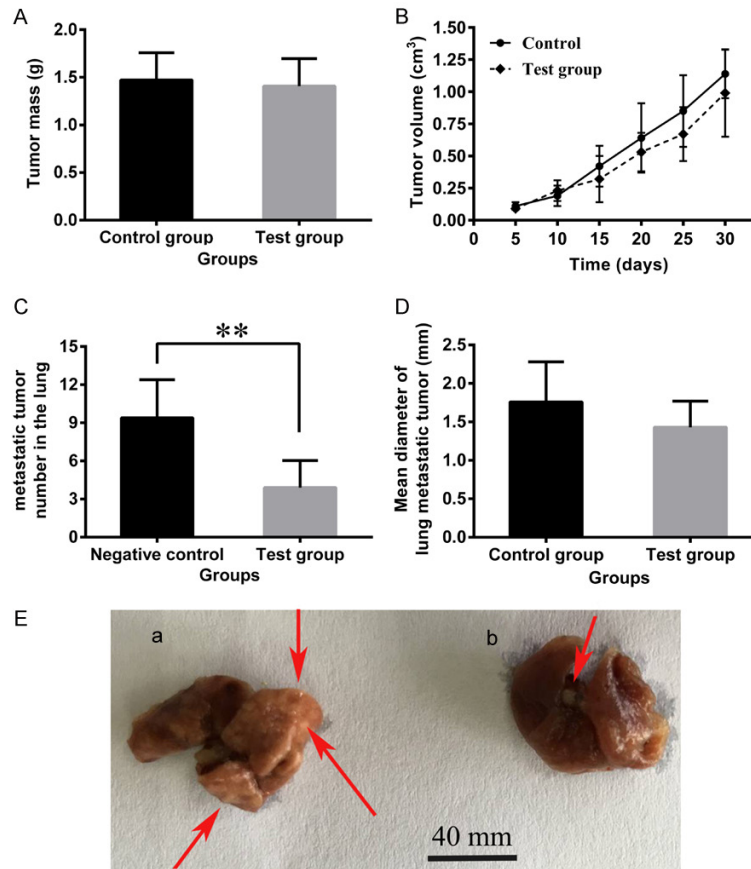


Figure 3. Inhibitory effects of metastin for (A) tumor mass and (B) tumor volume of subcutaneous transplanted tumors in nude mice. There were no significant differences in the tumor mass and tumor volume between the negative control and test groups; (C) Inhibitory effects of metastin on lung metastatic foci. There were significant differences in the average number of lung metastatic tumors between the negative control and test groups ($p < 0.01$); (D) There were no significant differences in the mean diameter of lung metastatic tumors between the negative control and test groups; (E) Inhibitory effects of metastin on lung metastatic foci after inoculation of SUNE-1-5-8F cells. (a) Metastin treatment group; (b) Negative control group. The red arrow indicates the metastatic tumor in the whole lung. ** indicates $p < 0.01$.

using an optical microscope. The maximum number and longest diameter of the lung metastatic tumors in the test group were 7 and 2.3 mm, respectively. Moreover, the maximum number and longest diameter of the lung metastatic tumors in the negative group were 16 and 2.8 mm, respectively. The average number of lung metastatic tumors was 9.4 for the negative control group and 3.9 for the test group. After comparing the average number of lung metastatic tumors between the test and negative control groups, it was found that the metastatic inhibition rate of metastin was 58.5%. There were significant differences in the numbers of lung metastatic tumors be-

tween the two groups ($p < 0.01$) (Figure 3C). The average diameter of the lung metastatic tumors was 1.76 for the negative control group and 1.43 for the test group. There were no significant differences in mean diameters of the lung metastatic tumors (Figure 3D, 3E).

Effects of metastin on survival of mice inoculated with SUNE-1-5-8F cells

After treating the mice bearing SUNE-1-5-8F cells with metastin, the average survival time was 56.40 ± 7.03 days. The average survival rate of the control mice was 39.40 ± 6.31 days. The average survival rate of the test group was 58.5% longer than that of the control group ($p < 0.05$). Moreover, the survival time of mice treated with metastin was 17 days longer than that of untreated mice. The two survival curves were separated after 30 days (Figure 4A). Present findings indicate that metastin exerts significant anti-tumor effects.

Hematoxylin-eosin staining and immunohistochemical staining of lung metastatic tumors

Metastatic tumor cells showed various sizes and different morphologies, as observed by hematoxylin-eosin staining. The nuclei were enlarged, with increased mitotic counts and pathological mitosis (Figure 4B). Immunohistochemical staining indicated strong positive expression of kisspeptin in the metastin treatment group, in contrast to weak expression levels of kisspeptin in the control group (Figure 4B).

Discussion

Migration, one of the most important biological behaviors of tumors, is closely associated

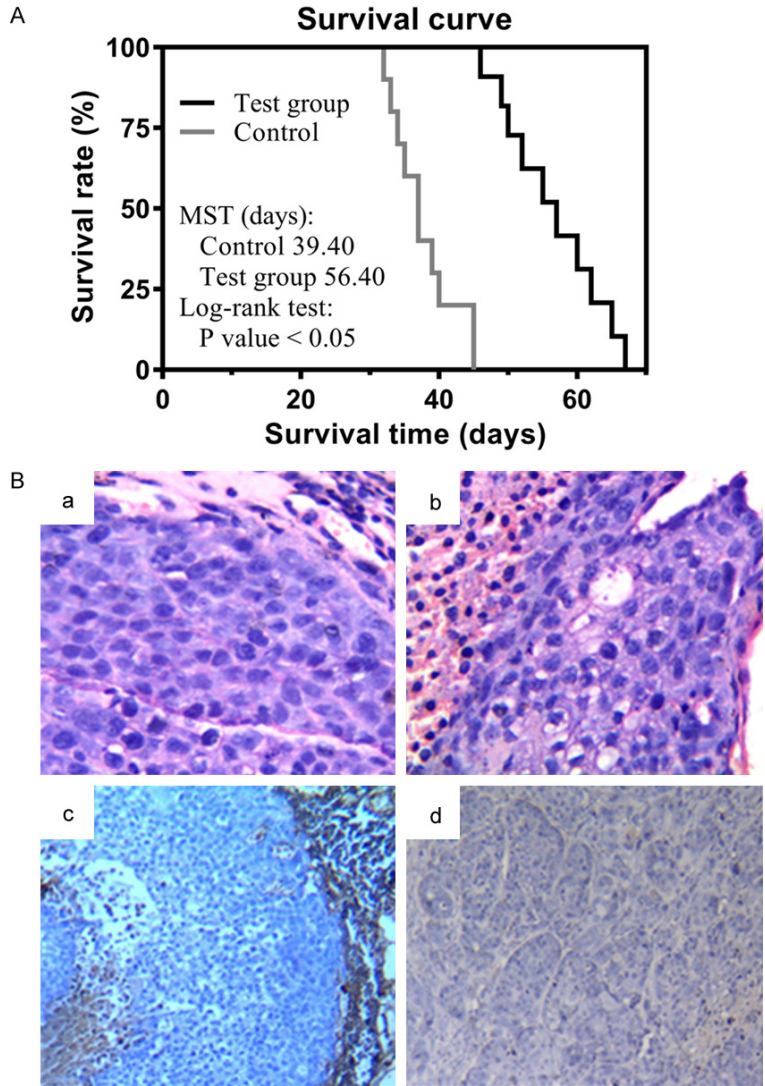


Figure 4. (A) Effects of metastatin on the survival curve of mice inoculated with SUNE-1-5-8F cells (MST, mean survival time); (B) Hematoxylin-eosin staining of lung metastatic tumors in the (a) metastatin treatment group and (b) negative control group. Immunohistochemical staining of lung metastatic tumors in the (c) metastatin treatment group and (d) negative control group.

low kisspeptin expression was far higher than that in patients with high kisspeptin expression ($p < 0.05$). Moreover, those with high kisspeptin expression had higher five-year survival rates. Kang et al. demonstrated that metastatin can inhibit the distant metastasis of endometrial cancer cells by binding to GPR54 [29]. In addition, GPR54 expression levels were closely associated with FIGO staging, grading, and deep myometrium ($p < 0.05$). Zhang et al. used immunohistochemistry for paired tumors and adjacent non-tumor tissues from 40 patients with osteosarcoma [30]. They illustrated that KISS-1 expression in tumor tissues was significantly lower than that in adjacent non-tumor tissues. Moreover, KISS-1 expression negatively correlated with distant metastasis ($p < 0.05$). KISS-1 inhibited tumor cell migration and invasion by regulating p38 MAPK and MMP-9. Although metastatin can inhibit migration and invasion of many tumor cells, the regulatory mechanisms remain unknown. Understanding the mechanisms of metastatic suppression is critical in reducing rates of distant metastasis and improving outcomes of lung tumors.

with angiogenesis and invasiveness [25, 26]. Migration is regulated by multiple genes. KISS-1 has recently been identified as a metastasis suppressor gene [27]. The 54 amino acids at the carboxyl terminal (68-121) of kisspeptin, which is encoded by KISS-1, are known as metastatin. Metastatin has been found to provide inhibitory effects on the migration of many tumor cells. Zhu et al. analyzed expression levels of kisspeptin and its ligand in 55 patients with liver metastases from colorectal cancer using immunohistochemistry [28]. They reported that the rate of distant metastasis in patients with

Metastatin inhibits migration and invasion of tumor cells by downregulating matrix metalloprotein-9 (MMP-9) expression. Migratory tumor cells must pass through the extracellular matrix. The main function of MMP-9 is to maintain a balance between degradation and remodeling of the extracellular matrix. Therefore, increased MMP-9 expression can promote metastasis. However, metastatin can reduce expression of MMP-9, inhibiting migration and invasion [31]. Chen et al. constructed a lentiviral vector pGC-LV-Kiss-EGFP and transfected it into colorectal cancer HCT116 cells, aiming to

induce overexpression of the KISS-1 gene [31]. As a result, the tumor suppressor protein I- κ B in NF- κ B signaling pathways was upregulated, while the downstream effector protein matrix metalloproteinase-9 (MMP-9) was downregulated. Therefore, MMP-9 can reduce cell adhesion, degrade the extracellular matrix, and promote metastasis [28].

Metastin also inhibits migration and invasion of tumor cells by inhibiting tumor angiogenesis. Tumor angiogenesis is the basis of tumor growth, invasion, and metastasis [32, 33]. Vascular endothelial growth factor-A (VEGF-A) is the most specific angiogenic factor of the VEGF family that can induce angiogenesis [34-37]. VEGF-A expression increases during tumor growth. Metastin can reduce expression of VEGF-A and inhibit growth, migration, and invasion of tumors [38, 39].

Several studies have proposed other inhibitory mechanisms of metastin on tumor metastasis: (1) Binding of metastin (kisspeptin-54, ligand) encoded by the KISS-1 gene to the receptor GPR54 encoded by the paired gene HOTAIR175 can activate phospholipase C, which is abundant in tumor cells. This leads to an increase of calcium ions in tumor cells, promoting differentiation and apoptosis [40]; (2) When GPR54 encoded by the HOTAIR175 gene is activated, expression of several adhesion factors that affect tumor metastasis is upregulated, inhibiting the migration of tumor cells; (3) Metastin can inhibit TNF α -Rho A-NF- κ B signaling pathways via paracrine and autocrine mechanisms, inhibiting gene transcription mediated by NF- κ B and migration and invasion of tumor cells [17, 24, 41].

In cell experiments, metastin has shown significant dose-dependent inhibitory effects on the human NPC SUNE-1-5-8F cell line ($p < 0.05$). Although metastin did not significantly inhibit the proliferation of tumor cells in the nude mouse model, it could reduce lung metastases ($p < 0.05$). This considerably prolonged the survival of mice ($p < 0.05$). In conclusion, metastin plays an important inhibitory role in the migration of NPC cells. Thus, metastin may offer a new solution, reducing distant metastases of tumors and prolonging survival times of tumor patients.

Acknowledgements

The present study was supported by the Anhui Provincial Natural Science Foundation (No. 140-8085MH190).

Disclosure of conflict of interest

None.

Address correspondence to: Hao Jiang, Department of Radiation Oncology, The First Affiliated Hospital of Bengbu Medical College and Tumor Hospital Affiliated to Bengbu Medical College, 287 Changhuai Road, Bengbu 233004, Anhui, P. R. China. E-mail: jianghao1223@163.com

References

- [1] Gossai NP, Naumann JA, Li NS, Zamora EA, Gordon DJ, Piccirilli JA and Gordon PM. Drug conjugated nanoparticles activated by cancer cell specific mRNA. *Oncotarget* 2016; 7: 38243-38256.
- [2] Chua MLK, Wee JTS, Hui EP and Chan ATC. Nasopharyngeal carcinoma. *The Lancet* 2016; 387: 1012-1024.
- [3] Ohtaki T, Shintani Y, Honda S, Matsumoto H, Hori A, Kanehashi K, Terao Y, Kumano S, Takatsu Y, Masuda Y, Ishibashi Y, Watanabe T, Asada M, Yamada T, Suenaga M, Kitada C, Usuki S, Kurokawa T, Onda H, Nishimura O and Fujino M. Metastasis suppressor gene KISS-1 encodes peptide ligand of a G-protein-coupled receptor. *Nature* 2001; 411: 613-617.
- [4] He Z, Wang Q, Sun Y, Shen M, Zhu M, Gu M, Wang Y and Duan Y. The biocompatibility evaluation of mPEG-PLGA-PLL copolymer and different LA/GA ratio effects for biocompatibility. *J Biomater Sci Polym Ed* 2014; 25: 943-964.
- [5] Kostakis ID, Agrogiannis G, Vaiopoulos AG, Mylona E, Patsouris E, Kouraklis G and Koutsilieris M. A clinicopathological analysis of KISS1 and KISS1R expression in colorectal cancer. *APMIS* 2015; 123: 629-637.
- [6] Shoji S, Nakano M, Tomonaga T, Kim H, Hanai K, Usui Y, Nagata Y, Miyazawa M, Sato H, Tang XY, Osamura YR, Uchida T, Terachi T and Takeya K. Value of metastin receptor immunohistochemistry in predicting metastasis after radical nephrectomy for pT1 clear cell renal cell carcinoma. *Clin Exp Metastasis* 2013; 30: 607-614.
- [7] Tan K, Cho SG, Luo W, Yi T, Wu X, Siwko S, Liu M and Yuan W. KISS1-Induced GPR54 signaling inhibits breast cancer cell migration and epithelial-mesenchymal transition via protein kinase D1. *Curr Mol Med* 2014; 14: 652-662.

Metastin inhibits migration and invasion of nasopharyngeal carcinoma cells

- [8] Savvidis C, Papaiconomou E, Petraki C, Msaouel P and Koutsilieris M. The role of KISS1/KISS1R system in tumor growth and invasion of differentiated thyroid cancer. *Anticancer Res* 2015; 35: 819-826.
- [9] Xie Y, Li Y, Peng X, Henderson F Jr, Deng L and Chen N. Ikappa B kinase alpha involvement in the development of nasopharyngeal carcinoma through a NF-kappaB-independent and ERK-dependent pathway. *Oral Oncol* 2013; 49: 1113-1120.
- [10] Su J, Xu XH, Huang Q, Lu MQ, Li DJ, Xue F, Yi F, Ren JH and Wu YP. Identification of cancer stem-like CD44+ cells in human nasopharyngeal carcinoma cell line. *Arch Med Res* 2011; 42: 15-21.
- [11] He Z, Huang J, Xu Y, Zhang X, Teng Y, Huang C, Wu Y, Zhang X, Zhang H and Sun W. Co-delivery of cisplatin and paclitaxel by folic acid conjugated amphiphilic PEG-PLGA copolymer nanoparticles for the treatment of non-small lung cancer. *Oncotarget* 2015; 6: 42150-42168.
- [12] Zhang S, Liu Q, Zhang Q and Liu L. MicroRNA-30a-5p suppresses proliferation, invasion and tumor growth of hepatocellular cancer cells via targeting FOXA1. *Oncol Lett* 2017; 14: 5018-5026.
- [13] Takeda T, Kikuchi E, Mikami S, Suzuki E, Matsumoto K, Miyajima A, Okada Y and Oya M. Prognostic role of KiSS-1 and possibility of therapeutic modality of metastin, the final peptide of the KiSS-1 gene, in urothelial carcinoma. *Mol Cancer Ther* 2012; 11: 853-863.
- [14] He Z, Shi Z, Sun W, Ma J, Xia J, Zhang X, Chen W and Huang J. Hemocompatibility of folic acid-conjugated amphiphilic PEG-PLGA copolymer nanoparticles for co-delivery of cisplatin and paclitaxel: treatment effects for non-small-cell lung cancer. *Tumour Biol* 2016; 37: 7809-7821.
- [15] Takayama-Ito M, Lim CK, Nakamichi K, Kakiuchi S, Horiya M, Posadas-Herrera G, Kurane I and Saijo M. Reduction of animal suffering in rabies vaccine potency testing by introduction of humane endpoints. *Biologicals* 2017; 46: 38-45.
- [16] Hankenson FC, Ruskoski N, van Saun M, Ying G-S, Oh J and Fraser NW. Weight loss and reduced body temperature determine humane endpoints in a mouse model of ocular herpesvirus infection. *J Am Assoc Lab Anim Sci* 2013; 52: 277-285.
- [17] Zhang Y, Pan J, Li H, Yu D, Wu T, Wang L, Wang Y, Zhou L and Zheng S. Albumin based nanomedicine for enhancing tacrolimus safety and lymphatic targeting efficiency. *J Biomed Nanotechnol* 2019; 15: 1313-1324.
- [18] Li Y, Zhao L, Xu X, Sun N, Qiao W, Xing Y, Shen M, Zhu M, Shi X and Zhao J. Design of (99mTc)-labeled low generation dendrimer-entrapped gold nanoparticles for targeted single photon emission computed tomography/computed tomography imaging of gliomas. *J Biomed Nanotechnol* 2019; 15: 1201-1212.
- [19] Martinez C, Vicente V, Yanez J, Alcaraz M, Castells MT, Canteras M, Benavente-Garcia O and Castillo J. The effect of the flavonoid diosmin, grape seed extract and red wine on the pulmonary metastatic B16F10 melanoma. *Histol Histopathol* 2005; 20: 1121-1129.
- [20] Smeda M, Przyborowski K, Proniewski B, Zakrzewska A, Kaczor D, Stojak M, Buczek E, Nieckarz Z, Zoladz JA, Wietrzyk J and Chlopicki S. Breast cancer pulmonary metastasis is increased in mice undertaking spontaneous physical training in the running wheel; a call for revising beneficial effects of exercise on cancer progression. *Am J Cancer Res* 2017; 7: 1926-1936.
- [21] Martinez C, Vicente V, Yanez MJ, Garcia JM, Canteras M and Alcaraz M. Experimental model of pulmonary metastasis treatment with IFN-alpha. *Cancer Lett* 2005; 225: 75-83.
- [22] Ahn J, Jeong J, Lee H, Sung MJ, Jung CH, Lee H, Hur J, Park JH, Jang YJ and Ha TY. Poly (lactico-glycolic acid) nanoparticles potentiate the protective effect of curcumin against bone loss in ovariectomized rats. *J Nanosci Nanotechnol* 2017; 13: 688-698.
- [23] Zhao X, Han Y, Zhu T, Feng N, Sun Y, Song Z, Li S, Liu J and Ding J. Electrospun polylactide-nano-hydroxyapatitevancomycin composite scaffolds for advanced osteomyelitis therapy. *J Biomed Nanotechnol* 2019; 15: 1213-1222.
- [24] Aparicio-Blanco J, Sebastian V, Rodriguez-Amaro M, Garcia-Diaz HC and Torres-Suarez AI. Size-tailored design of highly monodisperse lipid nanocapsules for drug delivery. *J Biomed Nanotechnol* 2019; 15: 1149-1161.
- [25] He Z, Sun Y, Cao J and Duan Y. Degradation behavior and biosafety studies of the mPEG-PLGA-PLL copolymer. *Phys Chem Chem Phys* 2016; 18: 11986-11999.
- [26] He Z, Sun Y, Wang Q, Shen M, Zhu M, Li F and Duan Y. Degradation and bio-safety evaluation of mPEG-PLGA-PLL copolymer-prepared nanoparticles. *J Phys Chem C Nanomater Interfaces* 2015; 119: 3348-3362.
- [27] Yin Y, Tang L and Shi L. The metastasis suppressor gene KISS-1 regulates osteosarcoma apoptosis and autophagy processes. *Mol Med Rep* 2017; 15: 1286-1290.
- [28] Zhu C, Takasu C, Morine Y, Bando Y, Ikemoto T, Saito Y, Yamada S, Imura S, Arakawa Y and Shimada M. KISS1 associates with better outcome via inhibiting matrix metalloproteinase-9 in colorectal liver metastasis. *Ann Surg Oncol* 2015; 22 Suppl 3: S1516-1523.

Metastin inhibits migration and invasion of nasopharyngeal carcinoma cells

- [29] Kang HS, Baba T, Mandai M, Matsumura N, Hamanishi J, Kharma B, Kondoh E, Yoshioka Y, Oishi S, Fujii N, Murphy SK and Konishi I. GPR54 is a target for suppression of metastasis in endometrial cancer. *Mol Cancer Ther* 2011; 10: 580-590.
- [30] Zhang Y, Tang YJ, Li ZH, Pan F, Huang K and Xu GH. KiSS1 inhibits growth and invasion of osteosarcoma cells through inhibition of the MAPK pathway. *Eur J Histochem* 2013; 57: e30.
- [31] Chen S, Chen W, Zhang X, Lin S and Chen Z. Overexpression of KiSS-1 reduces colorectal cancer cell invasion by downregulating MMP-9 via blocking PI3K/Akt/NF-kappaB signal pathway. *Int J Oncol* 2016; 48: 1391-1398.
- [32] Cao Y, Liang X, Li L, Pan R, Wang K, Xiao C, Li Z and Li P. High-efficiency EpCAM/EGFR-PLGA immunomagnetic beads with specific recognition on circulating tumor cells in colorectal cancer. *J Biomed Nanotechnol* 2017; 13: 758-766.
- [33] He Y, Guo T, Wang J, Sun Y, Guan H, Wu S and Peng X. Which induction chemotherapy regimen followed by cisplatin-based concurrent chemoradiotherapy is the best choice among PF, TP and TPF for locoregionally advanced nasopharyngeal carcinoma? *Ann Transl Med* 2019; 7: 104.
- [34] Jang K, Kim M, Gilbert CA, Simpkins F, Ince TA and Slingerland JM. VEGFA activates an epigenetic pathway upregulating ovarian cancer-initiating cells. *EMBO Mol Med* 2017; 9: 304-318.
- [35] He Z, Zhang X, Huang J, Wu Y, Huang X, Chen J, Xia J, Jiang H, Ma J and Wu J. Immune activity and biodistribution of polypeptide K237 and folic acid conjugated amphiphilic PEG-PLGA copolymer nanoparticles radiolabeled with ^{99m}Tc. *Oncotarget* 2016; 7: 76635-76646.
- [36] Bionas A, Giakoumettis D, Klonou A, Neromyliotis E, Karydakis P and Themistocleous MS. Paediatric gliomas: diagnosis, molecular biology and management. *Ann Transl Med* 2018; 6: 251.
- [37] Tsironis G, Ziogas DC, Kyriazoglou A, Lykka M, Koutsoukos K, Bamias A and Dimopoulos MA. Breakthroughs in the treatment of advanced squamous-cell NSCLC: not the neglected sibling anymore? *Ann Transl Med* 2018; 6: 143.
- [38] Shin WJ, Cho YA, Kang KR, Kim JH, Hong SD, Lee JI, Hong SP and Yoon HJ. KiSS-1 expression in oral squamous cell carcinoma and its prognostic significance. *APMIS* 2016; 124: 291-298.
- [39] Huang J, Zhang X, Wu Z, Wu Y, Wu X, Wang Y, Jiang H, Ma J, He Z. Preparation and biocompatibility evaluation of PEG-PLL/RGD-PEG-DSPC/phospholipid/CaP nanoparticles. *J Biomed Nanotechnol* 2018; 14: 98-113.
- [40] Tan YK, Liu KJ, Zou H, Yao HL, Jin JY, Zhang CY, Li QZ, Xiong L, Lei SL and Chen W. Inhibitory effect and molecular mechanism of the new porphyrin-based HCE6 photosensitizer on the activity of MKN45 human gastric cancer cells. *J Biomed Nanotechnol* 2019; 15: 1345-1353.
- [41] Arunraj TR, Rejinold SN, Mangalathillam S, Saroj S, Biswas R and Jayakumar R. Synthesis, characterization and biological activities of curcumin nanospheres (Journal of Biomedical Nanotechnology, Vol. 10(2), pp. 238-250 (2014)). *J Biomed Nanotechnol* 2019; 15: 1355-1356.